

*Title:*

## **Electromagnetic Modeling Of Beam Position Monitors For SNS Linac**

*Author(s):*

**Sergey S. Kurennoy and R.E. Shafer**

*Submitted to:*

**Proceed. of EPAC2000, Vienna, 2000, p.1768.**

<http://lib-www.lanl.gov/la-pubs/00818545.pdf>

# ELECTROMAGNETIC MODELING OF BEAM POSITION MONITORS FOR SNS LINAC

S.S. Kurennoy and R.E. Shafer, LANL, MS H824, Los Alamos, NM 87545, USA

## Abstract

Electromagnetic modeling of the beam position monitors (BPMs) for the Spallation Neutron Source (SNS) linac has been performed with MAFIA. The signal amplitudes and phases on the BPM electrodes are computed as functions of the beam transverse position using time-domain 3-D simulations with an ultra-relativistic beam. An analytical model is then applied to extrapolate the results to lower beam velocities. Based on the analysis results, an optimal BPM design with 4 one-end-shortened 60-degree electrodes has been chosen. It provides a very good linearity and sufficient signal power for both position and phase measurements, while satisfying the linac geometrical constraints and mechanical requirements.

## 1 INTRODUCTION

Beam position monitors (BPMs) in the SNS linac will deliver information about both the transverse position of the beam and the beam phase. Typical values for the beam position accuracy are on the order of 0.1 mm within 1/3 of the bore radius  $r_b$  from the axis ( $r_b$  is between 1 cm and 2 cm for the normal conducting part of the linac). The SNS linac BPMs will also serve as beam phase detectors, see [1] for details. The BPMs have a high signal processing frequency, equal to the microbunch repetition frequency in the linac,  $f_b=402.5$  MHz (or one of its lowest harmonics). A rather limited length along the beam line is available for BPM transducers, as usually in ion linacs, especially at low beam energies. This imposes certain restrictions on the linac BPM design.

To study options for the transducers of the SNS linac BPMs, we use the EM code MAFIA [2]. Electrostatic 2-D computations are used to adjust the BPM cross-section parameters to have 50- $\Omega$  transmission lines. Then 3-D static and time-domain computations are applied to calculate the electrode coupling. Time-domain 3-D simulations with an SNS beam microbunch passing through the BPM at a varying offset from the axis are used to compute the induced voltages on the electrodes as functions of time. After that an FFT procedure extracts the amplitudes and phases of the signal harmonics at individual outputs, as well as the amplitude and phase of the combined (summed) signal, versus the beam transverse position.

## 2 MAFIA MODEL OF BPM

To conform the restrictions mentioned above, it was decided to choose 4-electrode BPM design having stripline electrodes with one end shorted. A MAFIA model of the BPM consists of a cylindrical enclosure (box) with 4 electrodes on a beam pipe, see Fig. 1. The electrodes are flush with the beam pipe, shorted at one end, and have 50- $\Omega$  connectors on the other end. The beam pipe radius in the model is  $r_b=20$  mm, the electrode length along the beam is 40 mm, and their subtended angle is 60°. The 50- $\Omega$  terminations of the electrodes are modeled by discrete elements, 50- $\Omega$  resistors in this case.

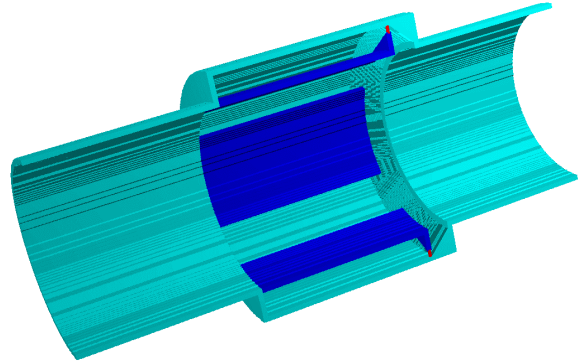


Figure 1: BPM model (1/2-cutout) with cone-tapered box end and electrodes (dark) with ridges near connectors.

This design provides a rigid mechanical structure with a good repeatability from one device to another, so that detailed mappings is required for a few BPMs only. The design is non-directional, which is useful in tight spots. It also eliminates four connectors, and since the remaining four are all on one end, the BPM can be mounted close to quadrupoles. The disadvantage of the one-end-shortened electrodes is the difficulty of their proper matching with a 50- $\Omega$  cable, as compared to stripline electrodes having 50- $\Omega$  connectors on both ends. The signal power in a BPM transducer for a given beam current can be increased by increasing the length and width of the electrodes (lobes). The electrode length is limited by available space on the beam line, in some cases as short as 5 cm. Wider electrodes provide a better linearity, but as the gap separating them is getting smaller one can expect a noticeable coupling. Within these constraints, we have considered a few possible designs. The electrode coupling is first calculated in a static approximation by solving a 2-D electrostatic problem to find potentials on passive

electrodes with a given potential on an active one. A similar procedure is used to adjust the BPM cross section for the electrodes to form 50- $\Omega$  transmission lines. In the dynamical 3-D problem, a 402.5-MHz *sine*-voltage with the amplitude increasing to some level is fed into a connector of an active electrode, and induced voltages on the passive ones are calculated. In both cases, the coupling coefficients are defined as ratios of the potentials or voltage amplitudes:  $k_{12}=A_2/A_1$  for two adjacent electrodes, and  $k_{13}=A_3/A_1$  for two opposite ones. Inserting the separators – the metal ridges connected to the BPM box and filling the gap between the adjacent electrodes – reduces the static coupling approximately by factor of two. With the separators, the coupling of 60° electrodes is reduced to about that of 45° electrodes.

Direct 3D time-domain computations with an ultra relativistic ( $\beta=1$ ) bunch passing the structure at the axis or parallel to the axis have been performed for a few layouts of the BPM transducers. A Gaussian longitudinal charge distribution of the bunch with the total charge  $Q=0.14$  nC and the rms length  $\sigma=5$  mm, corresponding to the 56-mA current in the baseline SNS regime with 2-MW beam power at 60 Hz, was used in the simulations. The MAFIA time-domain code T3 at present cannot simulate the open (or waveguide) boundary conditions on the beam pipe ends for non-ultra relativistic ( $\beta<1$ ) beams. In Sect. 3, the ultra relativistic MAFIA results are used to fix parameters of an analytical model of the BPM at  $\beta=1$ , and then to derive results for  $\beta<1$  analytically. Table 1 summarizes some results for a few types of the BPM electrodes with 60° subtended angle and length 40 mm: the dynamic couplings  $k_{12}$  ( $k_{13}\approx 1/3k_{12}$ ), the maximal signal voltages  $V(t)$  on the electrodes, and the amplitude of the voltage 1<sup>st</sup> Fourier harmonic (402.5 MHz) from an on-axis beam.

Table 1: Comparison of electrode types

Electrode	$k_{12}$	$V_m(t), V$	$\tilde{A}_1, V$
Rectangular	0.036	12.5	0.189
Tapered end	0.036	13.9	0.245
Tapered + cone box end	0.037	14.0	0.244
Same + separators	0.017	11.5	0.161
Ridged end + cone box	0.051	18.0	0.255

One can see that the separators reduce the electrode coupling but at the same time the signal power decreases. Having 50- $\Omega$  connectors on both ends of the electrode also reduces the dynamical coupling, while the signal power is about the same as in the one-end-shortened design. However, such a design is more complicated and more expensive, as well as less reliable mechanically, compared to the one-end-shortened version.

To study the BPM linearity, we perform simulations with the beam bunch passing through the BPM at different transverse positions. Figure 2 shows the voltages on all four electrodes for the case of a beam displaced from the chamber axis, and their Fourier transforms, for the BPM

design with ridged electrode end (Fig. 1, and the last line in Tab. 1). Indices  $R, T, L, B$  here refer to the right, top, left and bottom electrodes. The Fourier spectra of the signals have first peaks near 2 GHz, that approximately corresponds to the wavelength  $\lambda/4=l$ . For this BPM design, at high beam energies the signal power at 402.5 MHz changes between +4.6 dBm and -12.3 dBm as the beam position moves within a rather wide range,  $\{x, y \in (-r_b/2, r_b/2)\}$ , i.e. the signal dynamical range is 16.9 dB.

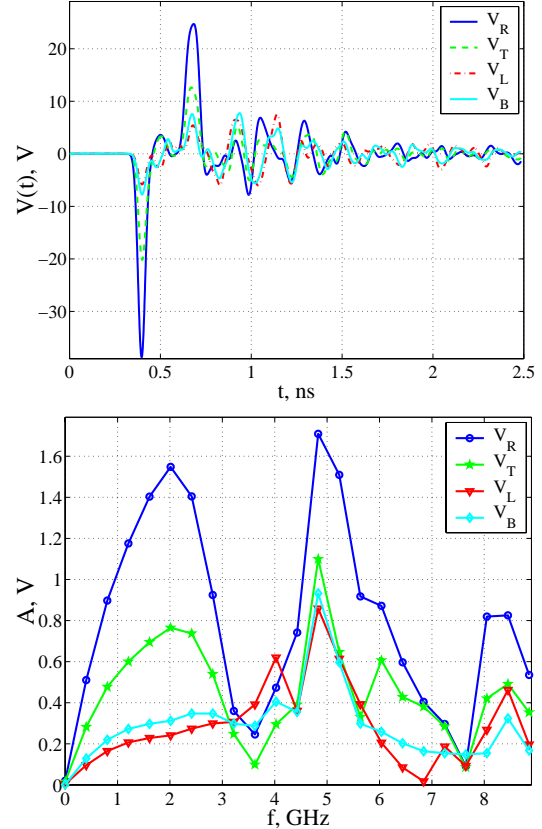


Figure 2: Signals on four BPM electrodes from a passing transversely displaced ( $x=r_b/2, y=r_b/4$ ) bunch:  
(a) voltages versus time for one period  $1/f_b=2.485$  ns;  
(b) normalized Fourier amplitudes (V) vs frequency.

The BPM linearity results are presented in Fig. 3. MAFIA data for the horizontal signal log ratio  $\ln(\tilde{A}_R/\tilde{A}_L)/2$  or the difference-over-sum  $(\tilde{A}_R - \tilde{A}_L)/(\tilde{A}_R + \tilde{A}_L)$  for different vertical beam positions overlap, so that it is difficult to distinguish between the five interpolating lines. One can conclude that the BPM design with 60° ridged electrodes (Fig. 1) is insensitive to the beam position in the direction orthogonal to the measured one, and has a good linearity. The BPM position sensitivity is equal to  $20\log_{10}(\tilde{A}_R/\tilde{A}_L)/x \approx 1.4$  dB/mm. As for other BPM designs considered, we have found that the linearity of BPMs with separators is much worse, in spite of the lower coupling.

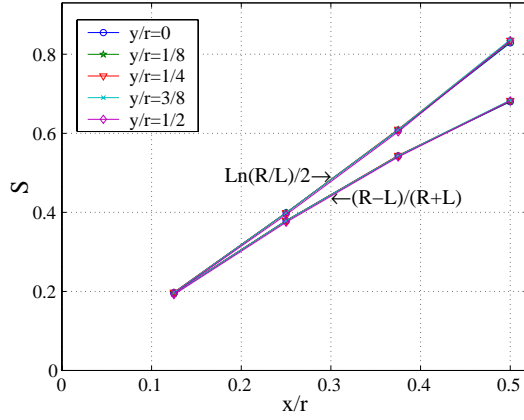


Figure 3: Signal ratio  $S$  at 402.5 MHz versus the beam horizontal displacement  $x/r_b$ , for a few values of the beam vertical displacement  $y/r_b$ .

### 3 ANALYTICAL MODEL OF BPM

Assuming an axial symmetry of the beam pipe, the signals on the BPM electrodes of inner radius  $r_b$  and angle  $\phi$  can be calculated by integrating induced currents within the electrode angular extent. For a pencil beam bunch passing the BPM at the transverse position  $x=rcos\theta$ ,  $y=rsin\theta$  at velocity  $v=\beta c$ , the signals are (e.g., [3]):

$$E(f, r, \theta) = C \frac{\varphi}{2\pi} \left[ \frac{I_0(g r)}{I_0(g r_b)} + \frac{4}{\varphi} \sum_{m=1}^{\infty} \frac{I_m(g r)}{I_m(g r_b)} \sin\left(m\left(\frac{\phi}{2} + \mu\right)\right) \cos(m(\theta - \nu)) \right], \quad (1)$$

where  $E=R, T, L, B$  are the Fourier components at frequency  $f$  of the voltages on the electrodes,  $(\mu, \nu)$  are  $(0, 0)$  for  $R$ ,  $(0, \pi/2)$  for  $T$ ,  $(\pi, 0)$  for  $L$ ,  $(\pi, \pi/2)$  for  $B$ , and  $I_m(z)$  are the modified Bessel functions. All dependence on frequency and energy is through  $g=2\pi f/(\beta\gamma c)$ , and overall coefficient  $C$  depends on the beam current. The parameters  $r_b$  and  $\varphi$  can be considered as “free” parameters of the model. Obviously, the induced current on an electrode in the real geometry is larger than an integral of the current density over the angle  $\phi$  in an axisymmetric pipe of radius  $r_b$ , since more electric field lines from a passing bunch end up on the electrode, compared to a circular pipe segment of the same radius and angular extent. We use Eqs. (1) to fit our MAFIA computation results for  $\beta=1$ , to find effective values of  $r_b$  and  $\varphi$ . One should expect these values to be larger than the geometrical ones.

Introducing the electrode coupling makes the model a bit more realistic. If  $k_{12}$  denotes the coupling coefficient between adjacent electrodes, and  $k_{13}$  between the opposite ones, the coupled signals (1) can be written as

$$R_c = [R + k_{12}(T + B) + k_{13}L] / (1 + 2k_{12} + k_{13}), \quad (2)$$

and similar for  $T_c, L_c, B_c$ , via cyclic permutations.

We fit the MAFIA results at 402.5 MHz for the ratio  $S/(x/r_b)$ , where  $S$  is either the log ratio  $\ln(\tilde{A}_R/\tilde{A}_L)/2$  or the difference-over-sum ratio  $(\tilde{A}_R - \tilde{A}_L)/(\tilde{A}_R + \tilde{A}_L)$ , with our model. The best fit to the numerical data was obtained with the effective parameters  $r_{\text{eff}}=1.17r_b$ ,  $\varphi_{\text{eff}}=1.24\varphi$  ( $=74.5^\circ$ ), where  $r_b=20$  mm,  $\varphi=\pi/3$  rad are the geometrical

values, and with  $k_{12}=k_{13}=0$ . It is interesting to note that the effective radius  $r_{\text{eff}}=23.4$  mm is close to the average of the electrode inner radius  $r_b=20$  mm and that of the BPM box, 26.5 mm, in agreement with earlier observations [4]. Attempts to introduce a non-zero coupling, even as small as 1%, lead to a rather wide spread between the curves for different  $y/r_b$ , so we have to conclude that the numerical results strongly suggest very small coupling between the BPM electrodes. This seems to contradict the dynamical coupling coefficients in Table 1. One should note, however, that Eq. (2) does not take into account that the inter-electrode coupling is mostly reactive, and  $ks$  in (2) should be complex, mostly imaginary.

Matching the amplitude of 402.5-MHz harmonics from an on-axis ultra relativistic SNS beam bunch with Eqs. (1) fixes the constant  $C=1.232$  V. The 402.5-MHz signal amplitudes for the displaced beams in Table 2 are then reproduced by the model with the accuracy of 1-2%. Assuming that these effective parameters of the model are applicable at lower beam velocities, we extrapolate  $\beta=1$  results to  $\beta<1$ . The signal power level for the on-axis beam is reduced by about 9 dB at  $\beta=0.073$  (2.5 MeV). For the strongest signal in the beam displacement range  $(-r_b/2, r_b/2)$  both vertically and horizontally, this reduction is 4.4 dB, and for the weakest one it is 12.9 dB. As a result, the dynamical range of the 402.5-MHz signal increases from about 17 dB for  $\beta=1$  to about 25 dB at  $\beta=0.073$ , if the same radius of BPM is assumed. Of course, at the low-energy end the bore and BPM radii are smaller, which increases the power level.

### 4 SUMMARY

Electromagnetic MAFIA modeling of the SNS linac BPMs has been performed. The signal amplitudes and phases on the BPM electrodes are computed as functions of the beam transverse position. Based on the analysis results, an optimal BPM design with 4 one-end-shortened 60-degree electrodes has been chosen. It provides a good linearity and sufficient signal power for both position and phase measurements, while satisfying the geometrical and mechanical requirements. Using the BPMs for accurate beam phase measurements is discussed in [1].

The authors acknowledge useful discussions with A.V. Aleksandrov, J.F. O’Hara, and J.F. Power.

### REFERENCES

- [1] S.S. Kurennoy, “Beam Phase Detectors for Spallation Neutron Source Linac”, these proceedings.
- [2] MAFIA Release 4.20, CST GmbH, Darmstadt, 1999.
- [3] R.E. Shafer, in AIP Conf. Proc. 319, 1994, p. 303.
- [4] R.E. Shafer, in AIP Conf. Proc. 212, 1990, p. 26.